JME

*J*ournal of *M*ining & *E*nvironment,
Vol.8, No.2, 2017, 227-235.
DOI: 10.22044/jme.2015.558

3D gravity data-space inversion with sparseness and bound constraints

M. Rezaie[1*], A. Moradzadeh[2] and A. Nejati Kalate[1]

1. School of Mining, Petroleum & Geophysics Engineering, Shahrood University of Technology, Shahrood, Iran
2. School of Mining Engineering, College of Engineering, University of Tehran, Tehran, Iran

Received 11 November 2015; received in revised form 26 December 2015; accepted 30 December 2015
**Corresponding author: mohammad1rezaie@gmail.com (M. Rezaie).*

Abstract
One of the most remarkable basis of the gravity data inversion is the recognition of sharp boundaries between an ore body and its host rocks during the interpretation step. Therefore, in this work, it is attempted to develop an inversion approach to determine a 3D density distribution that produces a given gravity anomaly. The subsurface model consists of a 3D rectangular prisms of known sizes and positions and unknown density contrasts that are required to be estimated. The proposed inversion scheme incorporates the Cauchy norm as a model norm that imposes sparseness and the depth weighting of the solution. A physical-bound constraint is enforced using a generic transformation of the model parameters. The inverse problem is posed in the data space, leading to a smaller dimensional linear system of equations to be solved and a reduction in the computation time. For more efficiency, the low-dimensional linear system of equations is solved using a fast iterative method such as Lanczos Bidiagonalization. The tests carried out on the synthetic data show that the sparse data-space inversion produces blocky and focused solutions. The results obtained for the 3D inversion of the field gravity data (Mobrun gravity data) indicate that the sparse data-space inversion could produce the density models consistent with the true structures.

Keywords: *Gravity Data, Data-Space Inversion, Sparseness Constraint, Bound Constraint, Lanczos Bidiagonalization, Mobrun.*

1. Introduction

Gravity measurements have been used in a wide range of investigations in geoscience, especially in mineral exploration [1-4]. Gravity-measured data are the vertical components of the Earth's gravitational field. The inversion of gravity data is an important step in the quantitative interpretation of the practical data since construction of the density contrast models significantly increases the amount of information that can be achieved using the gravity data [5]. Inversion is defined as a mathematical technique that automatically constructs a subsurface physical property model using the measured data by incorporating a priori information. The recovered models must be capable of predicting the measured data adequately [6]. Inversion of the potential field data such as gravity data suffers from non-uniqueness since, according to the Gauss's theorem, there are infinite equivalent source distributions that produce the same measured gravity field [7].

The standard approach used to obtain a unique solution is to use an additional (priori) information about the problem. The type and amount of the priori information must be determined to resolve the non-uniqueness of the solution [8]. There are numerous forms (geological, geophysical, and mathematical) of the priori information that enable us to incorporate information into the inversion process [9]. Some of them include the smooth and small model inversion [10, 5]; focused inversion [11, 12]; building models by growing source bodies [13]; inversion using different mathematical model forms [14]; covariance-based inversion [15]; stochastic lithology-based inversion [16];

structural inversion using linear programming [17]; inversion using an adaptive mesh [18]; data-space inversion with sparseness constraints [19]; and stochastic inversion using co-kriging [20].

In mineral exploration, one of the most remarkable basis of a potential field data interpretation concerns the detection of sharp boundaries between an ore body and its host rocks. Therefore, an algorithm producing a compact solution such as the focusing inversion algorithm, proposed by Zhdanov (2002) [21], and the one proposed by Pilkington (2008) [19] with sparseness constraints is the natural choice [9]. Data-space inversion with sparseness constraints was developed by Pilkington (2008) [19], originally for a 3D inversion of the magnetic data. In this algorithm, the solution is obtained with sparseness and just positivity constraints using the conjugate gradient iterative solver. The algorithm was modified later for a 3D inversion of the gravity data using a reference model [9].

In the 3D inversion of potential field data, a hard-constraint prior information of the physical property values is available. For instance, the physical property may be known to lie within particular bounds. We need to include this information into the inversion [22]. In the gravity inverse problem, bound constraint can improve the solution and make it more compact [23]. Therefore, implementation of negative bound constraint is necessary in the inversion of gravity data. In this case, modification of the current data-space inversion algorithm is necessary. It has been shown that Lanczos Bidiagonalization [24] is a faster iterative solver rather than the conjugate gradient (CG) method in the inversion of potential field data [25, 26].

In this work, at first, some modifications were applied on the algorithm of data-space inversion with sparseness constraints so that the general bound constraints can be applied for the 3D inversion of gravity data. For applying lower and upper bound constraints on the model parameters, a parameter transformation function that has previously been used in inversions for electrical conductivity and density data was applied [27, 28]. Then Lanczos Bidiagonalization was employed as a fast iterative solver in the 3D gravity data-space inversion with sparseness and bound constraints to speed up the required computation.

2. Methodology

To perform inverse modeling, the subsurface under the survey area is discretized into rectangular prisms of known sizes and positions. The density contrasts within each prism is an unknown parameter to be estimated by solving the inverse problem.

2.1 Forward modelling

Here, the formula given by Blakely (1996) [7] was used to compute the gravity response of each prism after discretization of the subsurface by rectangular prisms. If the observed gravity anomalies are caused by *n* subsurface rectangular prisms, the gravity anomaly at the *i*th field point is given by:

$$g_i = \sum_{j=1}^{n} G_{ij}\rho_j, \quad i = 1,\ldots,m \tag{1}$$

where g_i is the gravity observation at the *i*th point, ρ_j is the density contrast of the *j*th prism, and G_{ij} relates the *i*th datum of a unit density to the *j*th subsurface rectangular prism. In the matrix notation, Eq. (1) can be written as:

$$G\mathbf{m} = \mathbf{d}, G \in R^{m\times n}, \mathbf{d} \in R^{m}, \mathbf{m} \in R^{n} \tag{2}$$

Here, G is the forward operator matrix (also called the sensitivity matrix) that maps the physical parameters space into the data space. The vector $\mathbf{m}$ denotes unknown model parameters, and $\mathbf{d}$ is the data vector that is given by the measurements (g_i). There are some errors in the measurement data because of the noise that is assumed to be uncorrelated and have Gaussian distribution. Thus:

$$G\mathbf{m} = \mathbf{d} + \mathbf{e}, \quad \mathbf{e} \in R^{m} \tag{3}$$

where $\mathbf{e}$ is the vector of data error, and $\mathbf{d}_{obs} = \mathbf{d} + \mathbf{e}$ is the vector of observed data. The main purpose of the gravity inversion is to find a geologically credible density model (**m)** that predicts the measured data ($\mathbf{d}_{obs}$) at the noise level [29].

2.2 Inverse modelling

To achieve a solution to Eq. (3), minimization of the following total objective function (Φ) is required [19]:

$$\Phi = \left(\mathbf{d}_{obs} - G\mathbf{m}\right)^{T} D^{-1}\left(\mathbf{d}_{obs} - G\mathbf{m}\right) + C\left(\mathbf{m} - \mathbf{m}_0\right) \tag{4}$$

Expression D is the data weighting matrix given by $D^{-1} = \mathrm{diag}(1/\sigma_1,\ldots,1/\sigma_m)$, where σ_i stands for the standard deviation of the noise in

the *i*th datum, and $\mathbf{m}_0$ is the prior or starting model. The model objective function $C(\mathbf{m})$ comprises two parts, the depth-weighting function $Z(\mathbf{m})$ and a model norm term $P(\mathbf{m})$.

Due to the lack of depth resolution in the inversion of gravity data, a depth-weighting function was introduced by Li and Oldenburg (1998) [5]. It counteracts the spatial decay of the potential data with the depth by giving more weight to the rectangular prisms (cells) as depth increases.

$$Z(\mathbf{m}) = \frac{1}{z^{\beta}} \tag{5}$$

where z is the depth of each rectangular prism (cell), and β is equal to 3 in the magnetic case and to 2 in the gravity case [5, 10].

Sparseness is imposed on the model (**m**) using the Cauchy norm [30]:

$$P(\mathbf{m}) = \sum_{i=1}^{n} \ln\left(1 + m_i^2 / \eta^2\right) \tag{6}$$

where, m_i is the model parameter of the *i*th cell. The level of sparseness is controlled by the parameter η. $P(\mathbf{m})$ becomes small when more of the parameters m_i are smaller than η. This condition make the solution sparse and focused. If η is made large compared with all of the model parameters (**m**), then $P(\mathbf{m})$ has an effect similar to the minimum-norm solution, and has no influence on the sparseness of the model, and therefore, the model becomes smooth. Thus a judgment is required to determine an appropriate value for η for an inversion. This involves inspection of the solution visually and deciding whether it is geologically plausible [19].

The total objective function in Eq. (4) can be minimized in the data space by the model correction at iteration **k** as $\Delta\mathbf{m}_\mathbf{k}$ [31]:

$$\begin{aligned}\Delta\mathbf{m}_\mathbf{k} &= \mathbf{m}_\mathbf{k} - \mathbf{m}_\mathbf{0} = \\ &\alpha Q_k S_k^T G^T \left(G S_k Q_k S_k^T G^T + D\right)^{-1} \times \\ &\left(\mathbf{d}_{obs} - G\mathbf{m}_\mathbf{k} + G S_k \left[\mathbf{m}_\mathbf{k} - \mathbf{m}_\mathbf{0}\right]\right)\end{aligned} \tag{7}$$

where $\mathbf{m}_\mathbf{k}$ is the current model, and the constant α is a step length variable that is chosen so that each model correction is accepted only when the RMS error of fit is reduced. Initially, it is set to unity, and then it is reduced by a factor of 3 until a reduction in the fit is achieved. Q_k represents a diagonal matrix with elements $Q_{ii} = z_i^2\left(1 + m_i^2 / \eta^2\right)$, wherein z_i is the depth to the *i*th rectangular prism or voxel. Expression Q_k represents differentiating Eq. (6) with respect to the model parameters and imposes depth weighting and sparseness constraints. GS_k denotes the Jacobian matrix, where S_k is a diagonal matrix that imposes bound constraints (explained in the next section).

The forward problem is linear but comprising the model objective function and the parameter transformation leads to a non-linear problem that requires an iterative solution. The iterations proceed until the RMS misfit reaches an acceptable level or the model corrections become small enough [19]. For simplicity, we can write Eq. (7) in a compact form, as follows:

$$\Delta\mathbf{m}_\mathbf{k} = \alpha Q_k S_k^T G^T \mathbf{b}_k \tag{8}$$

where:

$$\begin{aligned}\mathbf{b}_k &= \left(G S_k Q_k S_k^T G^T + D\right)^{-1} \times \\ &\left(\mathbf{d}_{obs} - G\mathbf{m}_\mathbf{k} + G S_k \left[\mathbf{m}_\mathbf{k} - \mathbf{m}_\mathbf{0}\right]\right)\end{aligned} \tag{9}$$

For a large-scale problem, $\mathbf{b}_k$ is found at each iteration by solving an m × m inverse problem in Eq. (9) using the Lanczos Bidiagonalization method [24], as follows:

$$\mathbf{f}_k = A_k \mathbf{b}_k \tag{10}$$

where

$$A_k = \left(G S_k Q_k S_k^T G^T + D\right) \tag{11}$$

and

$$\mathbf{f}_k = \mathbf{d}_{obs} - G\mathbf{m}_\mathbf{k} + G S_k \left[\mathbf{m}_\mathbf{k} - \mathbf{m}_\mathbf{0}\right] \tag{12}$$

Iterative solvers algorithms provide very efficient tools for solving large and possibly ill-conditioned systems such as Eq. (10). The Lanczos Bidiagonalization and Conjugate Gradient methods are two iterative solvers that have been applied in the inversion of potential field data. However, the Lanczos Bidiagonalization method is faster and more efficient than the conjugate gradient method [22, 25, 26]. Therefore, we used the Lanczos Bidiagonalization method to obtain $\mathbf{b}_k$ in Eq. (10).

2.3. Physical bound constraints

Implementation of physical bound constraints can improve the results of inverse problems in potential field data, and is effective in reducing solution ambiguity [5, 10, 23]. Various techniques such as the logarithmic barrier approach [22], gradient projection approach [32], and transform function approach [19, 33, 34] have been applied in different inversion schemes to implement this constraint. Here, we preferred to apply the last method in the data space inversion algorithm to convert the physical property parameter to a generalized one $x = x(m)$. Then the inversion procedure can be solved with respect to vector $\mathbf{x}$ in the full numerical space, and the final-acquired model vector **m** is restricted in the given limits. There are many choices for the transform function, e.g. the logarithmic transform for positive constraints or the square function for non-negative constraints. We used a more generic transform to introduce the bound information, which can be written as [28]:

$$m_k(x) = \frac{a_k + c_k \exp(hx_k)}{1 + \exp(hx_k)} \qquad -\infty < x_k < \infty \qquad (13)$$

where a_k and c_k are the specified lower and upper limits for $m_k \in (a_k, c_k)$, respectively, and h is a variable controlling the steepness of the transformation. These parameters can be easily represented in the vector forms **a**, **c**, and **h** for the cases where bound information is provided for each cell in detail. Differentiating Eq. (13) with respect to x yields:

$$\frac{\partial m_k}{\partial x_k} = \frac{(c_k - a_k)\exp(hx_k)}{\left[1 + \exp(hx_k)\right]^2} \qquad (14)$$

This derivative is always positive and bounded [33]. For imposing bound constraints in Eq. (7), S_k is defined as a diagonal matrix with elements, $S_{ii} = \frac{(c_k - a_k)\exp(hx_k)}{\left[1 + \exp(hx_k)\right]^2}$. Therefore, at each iteration, Δx_k and x_k are calculated by solving Eq. (7), and then the bounded model parameters (m_k) can be achieved by Eq. (13).

3. Synthetic example

To evaluate the reliability of the introduced method, we inverted the synthetic gravity data of the model shown by Figure 1(a). This model is made by two different rectangular bodies (Table. 1), having a density of 1.0 g/cm^3. The density of uniform background was zero. The data was collected over an area of 1000 × 1000 m with a sample spacing of 25 m. There were 1600 data points that were contaminated by 3% of random noise.

The subsurface was discretized into 40 × 40 × 20 = 32000 rectangular prisms with a size of 25 m in the x, y, and z directions.

Table 1. Parameters of synthetic model.

Model number	x×y×z dimensions (m)	Depth to top (m)	True density (g/cm^3)
(1)	250×250×250	–50	1
(2)	500×125×200	–100	1

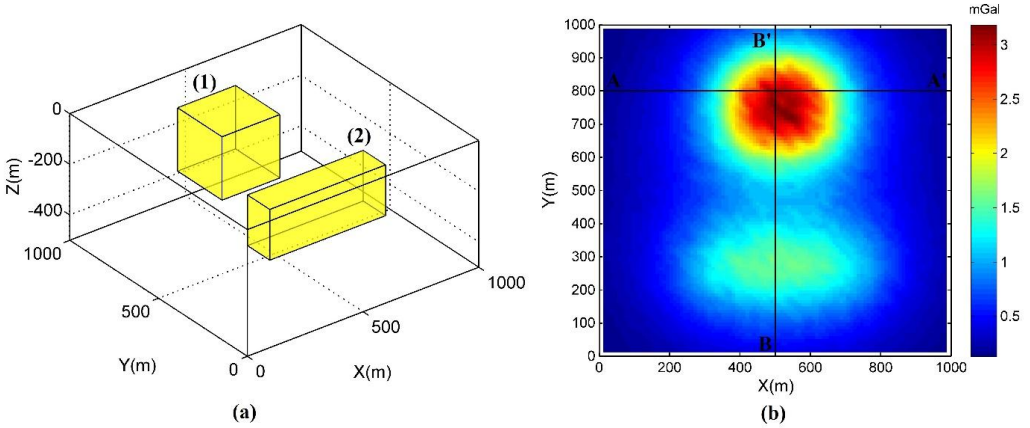

Figure 1. Perspective view of synthetic model (a). Gravity anomaly produced by synthetic model with 3% Gaussian noise (b).

The inverse problem was solved according to the procedure described in the preceding section. The maps of depth slices and cross sections through the recovered model from the sparse data space (h = 1 and $\eta = 0.05$) inversion algorithm are shown in Figure 2. The inversion used a starting model ($\mathbf{m}_0$) of zero, and yielded an RMS error of about 3%. Therefore, the result is acceptable with regard to the noise. The sparse solution is blocky, and defines two bodies precisely.

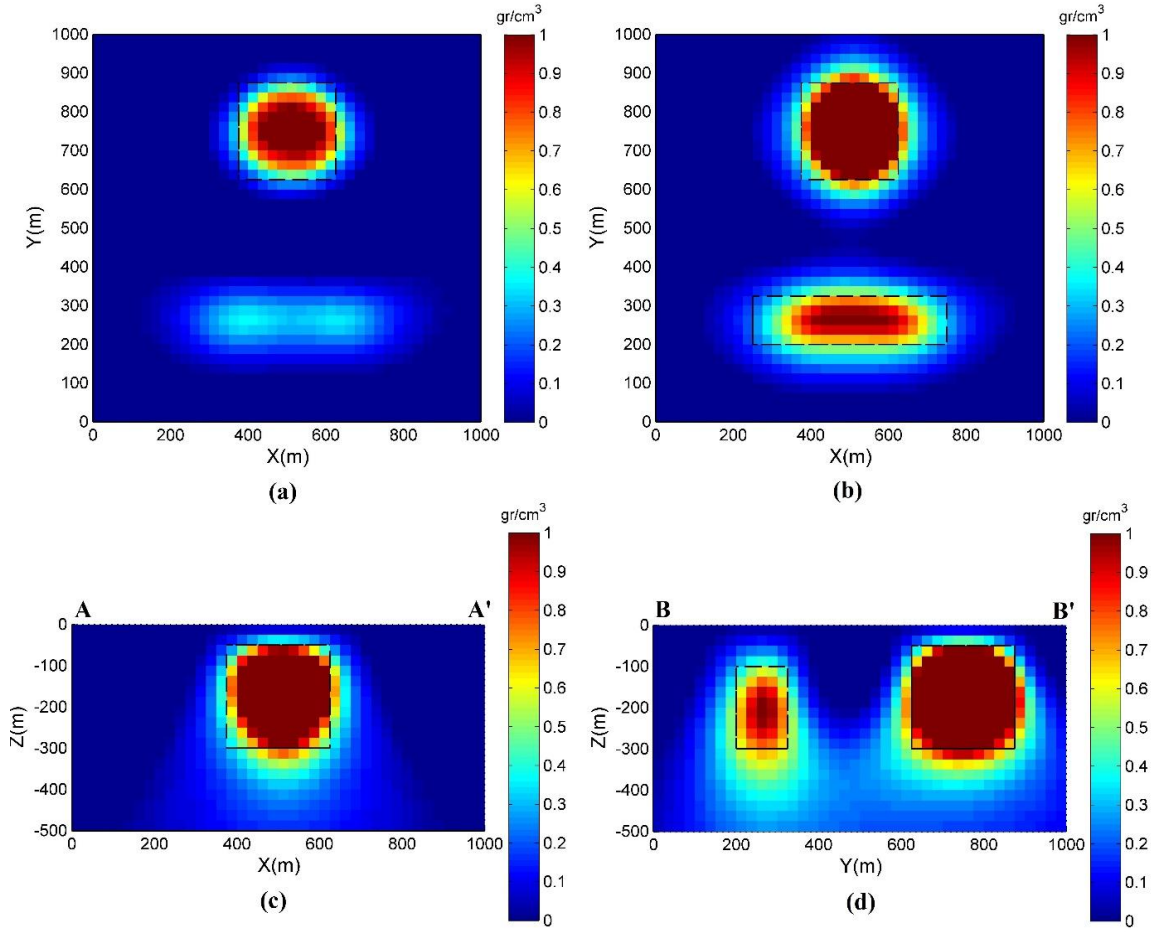

Figure 2. Plan sections through recovered density model obtained from inversion of gravity anomaly by the proposed method at z = –50 m (a) and z = –150 m (b). Cross-section slices of the density model at Y = 800 m (A-A') (c) and X = 500 m (B-B') (d).

Sparse solution defines the depths to the top and bottom of deep bodies adequately. However, the results obtained indicate acceptable reconstruction of the synthetic multisource anomaly at different depth levels below the surface and in vertical slices at Y = 800 m (A-A') and X = 500 m (B-B'). The recovered bodies in the model along these cross-sections are adequately matched with the real location of the synthetic bodies.

4. Application to field data

The developed inversion algorithm was applied to the field data acquired at the Mobrun sulfide body in Noranda, Quebec, Canada. The gravity anomaly is associated with a body of base metal massive sulfide, which has been hosted by volcanic rocks of middle Precambrian age. The density contrast of the orebody with host rock is about 1.9 (g/cm^3) [35]. The original gravity data was collected on 60 m spaced lines with stations of 30 m. The dataset consists of a regular grid of 38 × 33 data that is spaced 20 m× 20 m in the *x* and *y* directions, respectively. Figure 3(a) shows the gravity anomaly map constructed using the dataset.

For a 3D inversion of data, the subsurface of the studied area was discretized with 38 × 33 × 13 cells of 20 m in the *x*, *y*, and z directions, respectively. The data was inverted using the proposed algorithm with 0 g/cm^3 as the lower bound and 1.9 g/cm^3 as the upper bound.

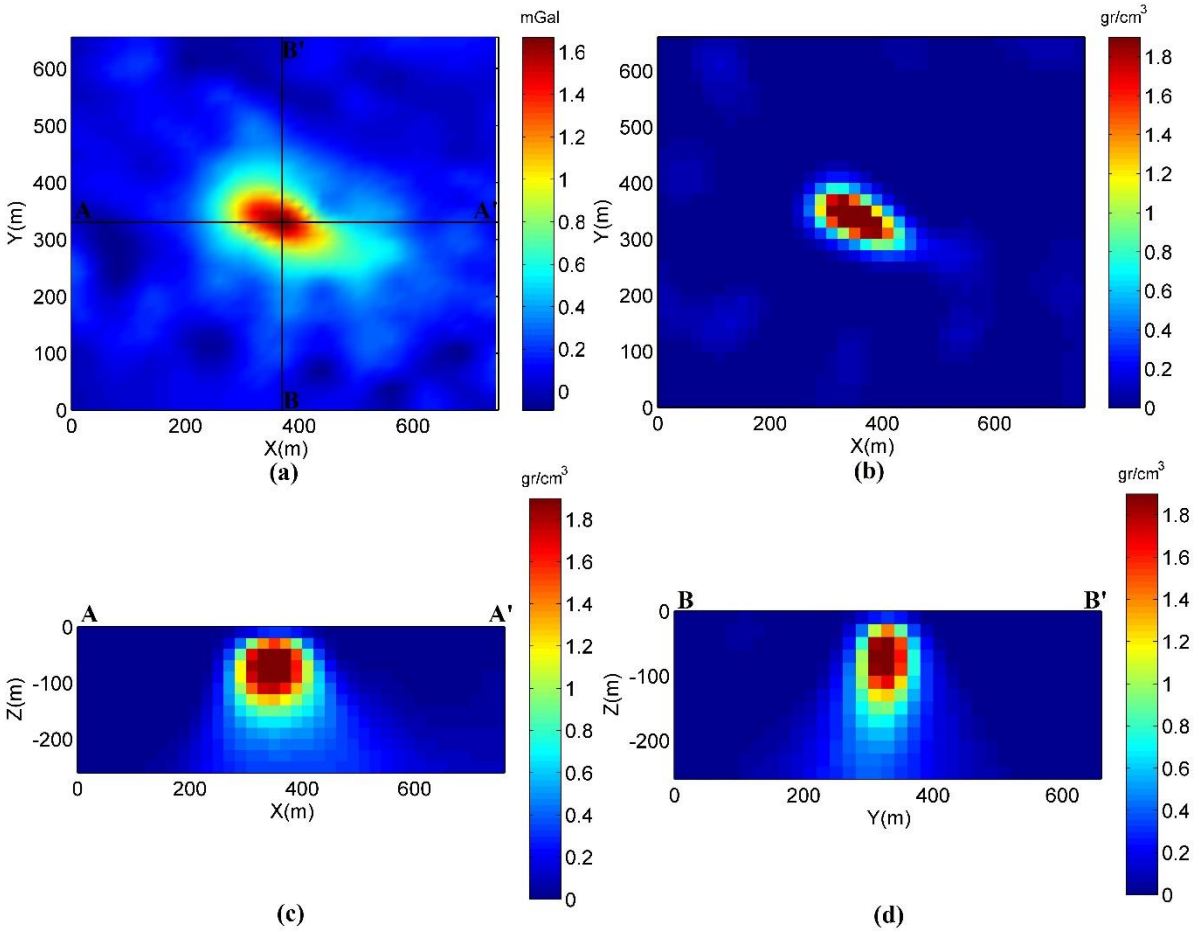

Figure 3. Bouguer anomaly map of Mobrun deposit (a), depth slice at Z = –45 m through recovered density model obtained from the inversion of gravity anomaly (b), cross-section slices of density model at Y = 330 m (B-B') (c), and X = 370 m (A-A') (d).

The depth slice map (at Z = –45 m) of the density model is shown in Figure 4(b), which shows that this sulfide body elongates from NW to SE. In Figure 4 (c and d), two cross-sections (at X = 370 m and Y = 330 m) of the recovered density model are shown. The 3D view of the inversion model for the Mobrun sulfide body considering a density cut off 0.8 g/cm^3 is shown in Figure 4.

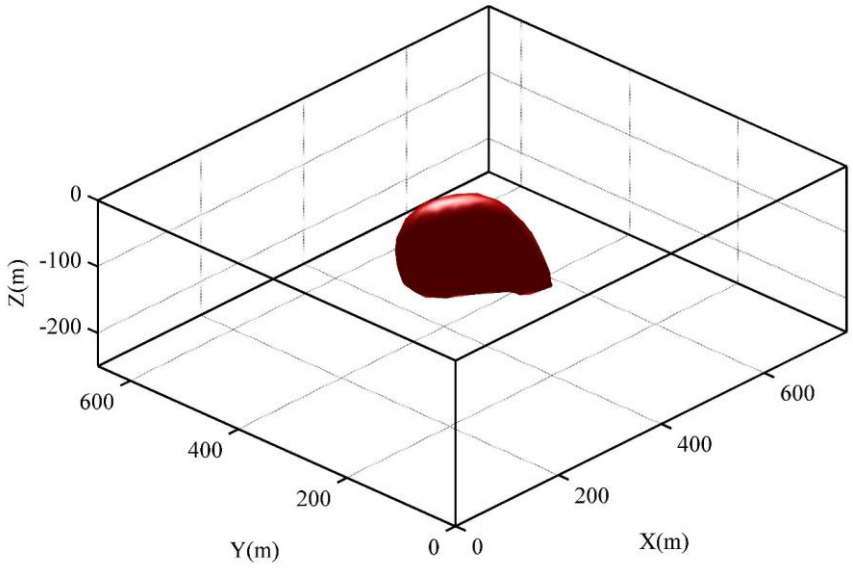

Figure 4. 3D view of inversion result at Mobrun sulfide body for a cut-off equal to 0.8 g/cm^3.

According to the results obtained, the depth to the top of the body was about 20 m, and it extended to the depth of more than 180 m. The location of the sulfide body and the mineralized zone were determined by drilling some boreholes. According to the drilling data, the depth to the top of body was about 17 m, and the ore body was extended to 187 m (Figure 5) [35]. Thus we obtained a good solution in agreement with the results of drilling and those obtained by Aghajani et al. (2009) [36].

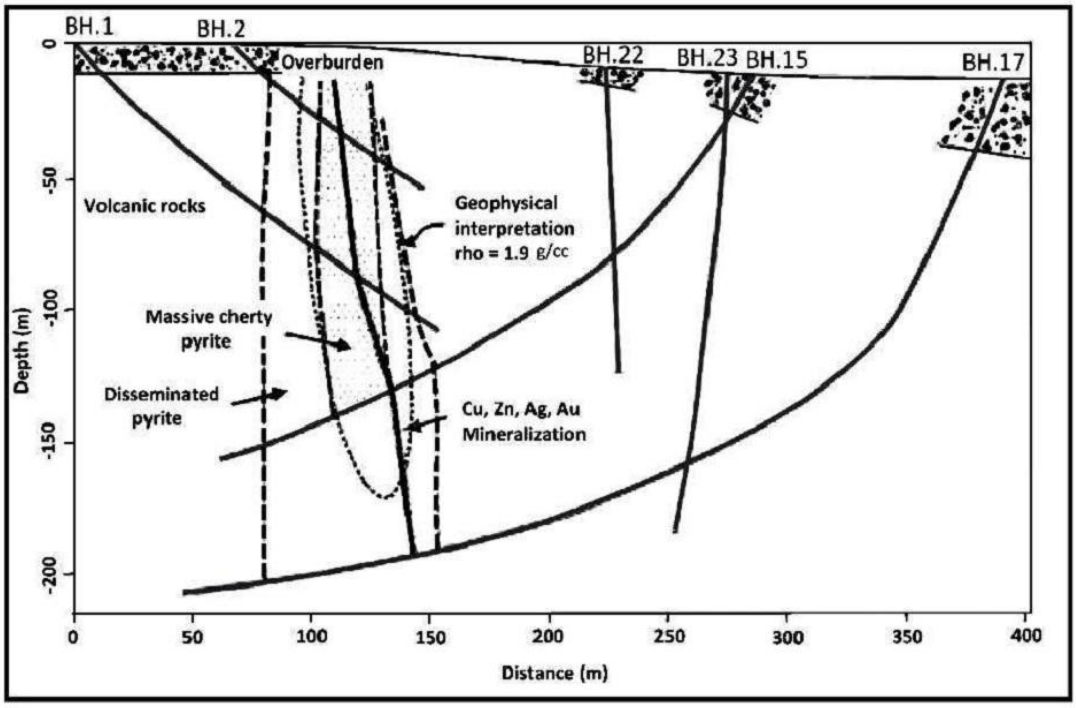

Figure 5. Center section of Mobrun sulfide body with geophysical interpretation [35].

5. Conclusions

We developed a 3D gravity data inversion approach that is capable of carrying out the optimization process in the *N*-dimensional data space, and incorporates a sparseness constraint. This leads to a smaller dimensional system of equations to be solved, and avoids the need for specifying any regularization parameter. Data space inversion leads to a significant reduction in the computation time compared with a model space approach because the number of data is usually less than the number of model parameters in a 3D gravity data inversion. This procedure further speeds up the inversion process using the fast Lanczos Bidiagonalization iterative algorithm. Addition of the Cauchy norm emphasizes the sparseness of the inverted model character. A logarithmic transformation was applied to impose bound constraints thorough the inversion process. A synthetic noise contaminated data test shows that the sparse, data-space gravity inversion produces a focused solution that defines the subsurface bodies precisely. Finally, the results of the 3D inversion of a real gravity data set from Mobrun sulfide body by the proposed inversion algorithm are in good agreement with those provided by the drilling and geological data.

References

[1]. Hinze, W.J. (1990). The role of gravity and magnetic methods in engineering and environmental studies. Geotechnical and environmental geophysics. 1: 75-126.

[2]. Hinze, W.J., Von Frese, R.B. and Saad, A.H. (2013). Gravity and Magnetic Exploration, Principles, Practices, and Applications. Cambridge University Press, 502 P.

[3]. Society of Exploration Geophysicists. (1990). Geotechnical and environmental geophysics (Vol. 1). In: S. H. Ward (Ed.). Tulsa, Oklahoma, pp. 147-189

[4]. Nabighian, M.N., Ander, M.E., Grauch, V.J.S., Hansen, R.O., Lafehr, T.R., Li, Y. and Ruder, M.E. (2005). 75th Anniversary Historical development of the gravity method in exploration. Geophysics. 70 (6): 63ND-89ND.

[5]. Li, Y. and Oldenburg, D.W. (1998). 3-D inversion of gravity data, Geophysics. 63 (1): 109-119.

[6]. Foks, N.L., Krahenbuhl, R. and Li, Y. (2014). Adaptive sampling of potential-field data : A direct approach to compressive inversion, Geophysics. 79 (1): IM1-IM9.

[7]. Blakely, R.J. (1996). Potential theory in gravity and magnetic applications, Cambridge University Press, 441 P.

[8]. Fedi, M., Hansen, P.C. and Paoletti, V. (2005). Analysis of depth resolution in potential-field inversion. Geophysics. 70 (6): A1-A11.

[9]. Marchetti, P., Coraggio, F., Gabbriellini, G., Ialongo, S. and Fedi, M. (2014). Large-scale 3D Gravity Data Space Inversion in Hydrocarbon Exploration. 84th Society of Exploration Geophysicists annual Meeting, Denver, USA, 26-31 October, 1269-1274.

[10]. Li, Y. and Oldenburg, D.W. (1996). 3-D inversion of magnetic data, Geophysics. 61 (2): 394-408.

[11]. Portniaguine, O. and Zhdanov, M.S. (1999). Focusing geophysical inversion images. Geophysics. 64 (3): 874-887.

[12]. Portniaguine, O. and Zhdanov, M.S. (2002). 3-D magnetic inversion with data compression and image focusing. Geophysics. 67 (5): 1532-1541.

[13]. Camacho, A.G., Montesinos, F.G. and Vieira, R. (2000). Gravity inversion by means of growing bodies. Geophysics. 65 (1): 95-101.

[14]. Boulanger, O. and Chouteau, M. (2001). Constraints in 3D gravity inversion. Geophysical Prospecting. 49 (2): 265-280.

[15]. Chasseriau, P. and Chouteau, M. (2003). 3D gravity inversion using a model of parameter covariance. Journal of applied geophysics. 52 (1): 59-74.

[16]. Guillen, A., Courrioux, G., Calcagno, P., Lane, R., Lees, T. and McInerney, P. (2004). Constrained gravity 3D litho-inversion applied to Broken Hill. ASEG Extended Abstracts. 2004 (1): 1-6.

[17]. Van Zon, T. and Roy-Chowdhury, K. (2006). Structural inversion of gravity data using linear programming. Geophysics. 71 (3): J41-J50.

[18]. Fullagar, P.K. and Pears, G.A. (2007). Towards geologically realistic inversion. In Proceeding of Exploration (Vol. 7), Fifth Decennial International Conference on Mineral Exploration, Toronto, Canada, 9-12 September, 7, 444-460.

[19]. Pilkington, M. (2008). 3D magnetic data-space inversion with sparseness constraints. Geophysics. 74 (1): L7-L15.

[20]. Shamsipour, P., Chouteau, M. and Marcotte, D. (2011). 3D stochastic inversion of magnetic data. Journal of Applied Geophysics. 73 (4): 336-347.

[21]. Zhdanov, M.S. (2002). Geophysical inverse theory and regularization problems (Vol. 36). Elsevier, Amsterdam, 609 P.

[22]. Li, Y. and Oldenburg, D.W. (2003). Fast inversion of large-scale magnetic data using wavelet transforms and a logarithmic barrier method. Geophysical Journal International. 152 (2): 251-265.

[23]. Oldenburg, D.W. and Li, Y. (2005). Inversion for applied geophysics: A tutorial. Investigations in geophysics. (13): 89-150.

[24]. Paige, C.C. and Saunders, M.A. (1982). LSQR: An algorithm for sparse linear equations and sparse least squares. ACM Transactions on Mathematical Software (TOMS). 8 (1): 43-71.

[25]. Abedi, M., Gholami, A., Norouzi, G-H. and Fathianpour, N. (2013). Fast inversion of magnetic data using Lanczos bidiagonalization method. Journal of Applied Geophysics. 90: 126-137.

[26]. Martin, R., Monteiller, V., Komatitsch, D., Jessell, M., Bonvalot, S. and Lindsay, M. (2013). Gravity inversion using wavelet-based compression on parallel hybrid CPU / GPU systems : application to southwest Ghana. Geophysical Journal International. 1594-1619.

[27]. Commer, M. and Newman, G.A. (2008). New advances in three-dimensional controlled-source electromagnetic inversion. Geophysical Journal International. 172 (2): 513-535.

[28]. Commer, M. (2011). Three-dimensional gravity modelling and focusing inversion using rectangular meshes. Geophysical Prospecting. 59 (5): 966-979.

[29]. Vatankhah, S., Ardestani, V.E. and Renaut, R.A. (2015). Application of the $\chi 2$ principle and unbiased predictive risk estimator for determining the regularization parameter in 3-D focusing gravity inversion. Geophysical Journal International. 200 (1): 265-277.

[30]. Sacchi, M.D. and Ulrych, T.J. (1995). High-resolution velocity gathers and offset space reconstruction. Geophysics. 60 (4): 1169-1177.

[31]. Tarantola, A. (1987). Inverse problem theory: Elsevier Science.

[32]. Lelièvre, P.G., Oldenburg, D.W. and Williams, N.C. (2009). Integrating geological and geophysical data through advanced constrained inversions. Exploration Geophysics. 40: 334-341.

[33]. Kim, H.J. and Kim, Y.H. (2008). Lower and upper bounding constraints of model parameters in inversion of geophysical data. Society of Exploration Geophysicists Annual Meeting, Las Vegas, USA, 9-14 November. 692-696.

[34]. Lelievre, P.G. and Oldenburg, D.W. (2006). Magnetic forward modelling and inversion for high

susceptibility. Geophysical Journal International. 166 (1): 76-90.

[35]. Grant, F.S. and West, G.F. (1965). Interpretation theory in applied geophysics. McGrawHill, New York.

[36]. Aghajani, H., Moradzadeh, A. and Zeng, H. (2009). Normalized full gradient of gravity anomaly method and its application to the Mobrun sulfide body, Canada. World Applied Sciences Journal. 6 (3): 393-400.

وارون‌سازی سه‌بعدی داده‌ای گرانی در فضای داده با قیدهای پراکندگی و کران محدود

محمد رضایی[۱*]، علی مرادزاده[۲] و علی نجاتی کلاته[۱]

۱- دانشکده مهندسی معدن، نفت و ژئوفیزیک، دانشگاه صنعتی شاهرود، ایران

۲- دانشکده فنی و مهندسی، دانشکده معدن، دانشگاه تهران، ایران

ارسال ۲۰۱۵/۱۱/۱۱، پذیرش ۲۰۱۵/۱۲/۳۰

* نویسنده مسئول مکاتبات: mohamad1rezaie@gmail.com

چکیده:

یکی از مهم‌ترین دلایل وارون‌سازی داده‌های گرانی در فرآیند تفسیر این داده‌ها، تشخیص دقیق مرزهای بین ماده معدنی و سنگ‌های دربرگیرنده است؛ بنابراین در این تحقیق سعی شده است که یک روش وارون‌سازی برای تعیین توزیع سه‌بعدی چگالی سنگ‌ها توسعه داده شود به‌گونه‌ای که ناهنجاری گرانی داده شده را بازسازی کند. مدل زیرسطحی از منشورهای سه‌بعدی مستطیلی تشکیل شده است که ابعاد و موقعیت آن‌ها مشخص است ولی اختلاف چگالی این منشورها نامعین بوده که باید تخمین زده شود. روش وارون‌سازی ارائه شده از نرم کوشی و تابع وزنی عمقی به عنوان نرم مدل استفاده کرده که قید پراکندگی را به جواب اعمال می‌کند. قید کران فیزیکی محدود از طریق تبدیل عمومی پارامترهای مدل اعمال می‌شود. مسئله وارون در فضای داده حل می‌شود، این کار باعث تشکیل سیستم معادلات خطی با ابعاد کمتر شده و زمان محاسبه کمتری نیاز دارد. برای کارایی بهتر، سیستم معادلات خطی کم بعد حاصله با استفاده از یک روش تکرار شونده سریع مثل روش دو قطری سازی لنکزوس حل می‌شود. آزمون‌های انجام گرفته روی داده‌های مصنوعی نشان می‌دهد که وارون‌سازی فضای داده جواب‌هایی بلوکی و متمرکز تولید می‌کند. نتایج به دست آمده از وارون‌سازی سه‌بعدی داده‌های گرانی واقعی (داده‌های گرانی موبرون) نشان می‌دهد که وارون‌سازی فضای داده پراکنده می‌تواند مدل توزیع چگالی را تولید کند که با ساختارهای واقعی همخوانی دارد.

کلمات کلیدی: داده گرانی، وارون‌سازی فضای داده، قید پراکندگی، قید کران، دو قطری سازی لنکزوس، موبرون.